Atomization and Sprays, 32(4):25–51 (2022)

EXPERIMENTAL INVESTIGATION OF EFFERVESCENT ATOMIZATION, PART II: INTERNAL FLOW AND SPRAY CHARACTERIZATION WITH NOVEL DARPA SUBOFF AFTERBODY STREAMLINE AERATOR

Andrew Niland,[1] R. Santhosh,[2,*] Richard Marsh,[1] & Philip Bowen[1]

[1]*Cardiff School of Engineering, Cardiff University, Wales CF24 3AA, UK*

[2]*Department of Mechanical Engineering, Indian Institute of Technology (BHU) Varanasi, Varanasi 221005, India*

*Address all correspondence to: R. Santhosh, Department of Mechanical Engineering, Indian Institute of Technology (BHU) Varanasi, Varanasi 221005, India, E-mail: rsanthosh.mec@iitbhu.ac.in

Original Manuscript Submitted: 6/7/2021; Final Draft Received: 11/14/2021

This experimental work reports, for the first time, observations of an internal flow field involving a DARPA SUBOFF afterbody design aerator body in an inside-out type of effervescent atomizer. The effect of operating parameters like air-to-liquid ratio (ALR), operating pressure, aerator orifice diameter, aeration area, and mixing chamber diameter on internal flow within the effervescent atomizer is studied. The effect of increasing ALR on the internal flow is quantified by identifying different gas injection mechanisms at the aerator orifice (into the mixing chamber) and two-phase mixing chamber flow regimes using high-speed shadowgraphy. In particular, it is observed that as ALR is systematically increased, the gas injection mechanism transits in the following sequence: single bubbling, pulsed bubbling, elongated jetting, atomized jetting, and evacuated chamber. The range of ALRs within which these mechanisms are observed are employed to draw up a flow regime map. Similar analysis on two-phase mixing chamber flow regimes yielded a corresponding regime map for internal two-phase stabilized flow in the mixing chamber. The flow regime transited from bubbly flow, to slug flow, to churn flow, and finally to annular flow as the ALR was increased. The spray characteristics (size and velocity) at the nozzle exit are reported using phase Doppler anemometry measurements. It is observed that dense-bubbly and bubbly-slug flow regimes produce stable sprays with droplet sizes in the range of 50–80 μm in the range of 0.25%–1.50% ALR.

KEY WORDS: *effervescent atomization, DARPA SUBOFF afterbody streamlined aerator, gas injection regime, internal flow regimes, aerator, mixing chamber design*

1. INTRODUCTION

The process of effervescent atomization represents shattering of the liquid core due to gas bubbles embedded in it caused by substantial pressure drop when the two-phase fluid is forced to

NOMENCLATURE

A_a	aeration area, m^2	OR_{bubbling}	bubbling operating range, g^2/s^2
A_{MC}	mixing chamber cross-sectional area, m^2	P_{op}	operating pressure (i.e., differential pressure between mixing chamber and atmosphere), bar
d_a	aerator orifice diameter, m		
d_{MC}	mixing chamber diameter, m		

exit through a narrow orifice (Lefebvre et al., 1988; Lefebvre, 1988; Roesler and Lefebvre, 1989; Wang et al., 1989).

Effervescent atomization performance is characterized by considering a number of parameters like internal flow characterization, bubble sizing, discharge coefficient, near-nozzle spray structure, spray cone angle, droplet sizing, droplet velocity, and so on (Loebker and Empie, 1997; Lefebvre et al., 1988; Roesler and Lefebvre, 1989; Panchagnula and Sojka, 1999; Chen and Lefebvre, 1994; Buckner and Sojka, 1993). While some of these performance parameters generate qualitative outcomes (e.g., internal flow determination, near nozzle spray structure), the majority can be quantified by measurable and comparable evaluates [e.g., bubble size, droplet Sauter mean diameter (SMD), and velocity]. The majority of these performance parameters have been shown to vary with a number of operating parameters like liquid mass flow rate, air-to-liquid ratio (ALR) or gas-to-liquid ratio, operating pressure, aerator design, mixing chamber design, exit orifice design, liquid properties, and so on.

The present work concerns characterization of flow inside the effervescent atomizer and study of its dependence on operating parameters like ALR, operating pressure, orifice diameter, and area and mixing chamber diameter. The internal flow is known to have a significant effect on the atomization mechanisms, where a bubbly flow is a prerequisite for effervescent atomization (Kim and Lee, 2001; Roesler and Lefebvre, 1988; Santangelo and Sojka, 1995; Buckner and Sojka, 1991). The study of internal flow is categorized into two types: the study of gas injection processes at the aerator body from its orifices and the visualization of stabilized gas-liquid flow in the mixing chamber. The results of internal flow visualizations are usually quantified by categorizing the internal flow behavior (both at the aerator orifice and in the mixing chamber) into flow regimes (Catlin and Swithenbank, 2001; Kim and Lee, 2001; Lörcher et al., 2005; Jobedhar, 2014; Hampel et al., 2009; Huang et al., 2008; Jedelsky and Jicha, 2013; Sun et al., 2015; Stähle et al., 2015a,b; Gomez, 2010; Lörcher and Mewes, 2001; Liu et al., 2010; Hang et al., 2014), with some researchers extending this analysis to produce flow maps (Kim and Lee, 2001; Huang et al., 2008; Stähle et al., 2015a; Lörcher and Mewes, 2001; Hang et al., 2014). Commonly, published flow maps are referenced between studies as a technique to predict the flow regimes in effervescent atomizers where internal flow measurement may not be possible. However, in many cases, the flow maps used originate from alternative research fields, and therefore the conditions could be unrepresentative of an effervescent atomizer (e.g., long residence time); consequently, their reliability for predicting effervescent atomizer internal flow regime could be questioned.

There is consensus across the literature that the ALR has a significant effect on effervescent atomization (Jedelsky et al., 2009; Petersen et al., 2001; Chin and Lefebvre, 1995; Lefebvre, 1996; Wang et al., 1989; Buckner and Sojka, 1991; Panchagnula and Sojka, 1999; Sutherland et al., 1997; Lefebvre et al., 1988), affecting both the internal flow and spray quality. Consequently,

it is the most common independent parameter examined throughout the literature. The dependence of the gas injection processes at the aerator on ALR is a severely underresearched area in effervescent atomization. Jobedhar (2014) performed a basic qualitative assessment of bubble formation at the aerator for an effervescent atomizer, in which only the aerator hole spacing was varied. Sen et al. (2014) observed the effects of downstream events on bubble formation at the aerator, but their investigation was limited to a sparse bubbly flow and featured an unrepresentative atomizer design for real-world application (i.e., square cross-section mixing chamber, 1.12 m mixing length, 0.017% ALR). However, no researcher has identified the gas injection regimes at the aerator, and therefore the relationship between the gas injection regimes at the aerator and the flow regime generated within the mixing chamber has not been established; this restricts comparability between aerator studies in alternative research fields (e.g., nuclear, waste treatment) for effervescent atomization. Despite the notable lack of research at the aerator, the effect of ALR on the internal flow regimes within the mixing chamber has been well evidenced in effervescent atomization literature. Increasing the ALR is widely reported to transition the internal flow regime from bubbly flow, to intermittent regimes (e.g., slug flow, churn flow), and finally to annular flow (Lefebvre, 1996; Jobedhar, 2014; Huang et al., 2008; Stähle et al., 2015a; Chin and Lefebvre, 1993). Generally, low ALRs are associated with small, discrete bubbles in the mixing chamber (i.e., bubbly flow) (Huang et al., 2008). The bubble size and/or number is observed to increase with ALR (Lefebvre, 1996; Jobedhar, 2014; Chin and Lefebvre, 1993), and hence the frequency of bubble coalescence increases, eventually forming large gas slugs in the flow and instigating formation of intermittent flow regimes (e.g., slug flow, churn flow). This corresponds to experimental studies that report increased instability at 2% ALR (Santangelo and Sojka; 1995), 3% ALR (Liu et al., 2010), and 5% ALR (Sun et al., 2015; Sovani et al., 2001), which is thought to represent the critical ALRs at which transition between bubbly flow and slug flow occurs. At high ALRs, the internal flow transitions to a fully annular flow (Rahman et al., 2012; Huang et al., 2002); this is reported to occur between 5% ALR (Santangelo and Sojka; 1995; Sun et al., 2015; Sovani et al., 2005) and 10% ALR (Mlkvik et al., 2015), with diminishing effects of ALR above 20% ALR (Sojka and Lefebvre, 1990). As a result of these differing internal flow regimes, the gas-phase expansion mechanisms have also been shown to vary from single bubbling to tree regime with increasing ALR, which results in a decrease in atomizer efficiency (Sojka and Lefebvre, 1990; Jedelsky and Jicha, 2013).

This two-phase flow is then supplied to the exit orifice, where the presence of a gas phase restricts the liquid flow area. The addition of further gas promotes this restriction, hence the coefficient of discharge is reported to decay with an increasing ALR (Lefebvre, 1988b; Jedelsky et al., 2003, 2009; Chin and Lefebvre, 1995; Schröder et al., 2011; Ochowiak et al., 2010; Lefebvre and Chen, 1994; Ramamurthi et al., 2009). Hence, the use of increasing the atomizing gas flow rate to achieve atomizer turndown is most effective at low ALRs.

It is unanimously agreed across the literature that the droplet SMD decreases with increasing ALR (Lefebvre, 1988b; Sojka and Lefebvre, 1990; Catlin and Swithenbank, 2001; Konstantinov, 2012; Jedelsky et al., 2009; Kim and Lee, 2001; Nielsen et al., 2006; Petersen et al., 2001; Jobehdar, 2014; Huang et al., 2008, 2011; Schröder et al., 2011, 2012; Geckler et al., 2008; Broniarz-Press et al., 2010; Ochowiak et al., 2012; Ma et al., 2013; Ochowiak, 2012), particularly in the spray centerline (Jedelsky et al., 2009; Schröder et al., 2012). An increase in ALR acts to reduce the liquid film thickness in the exit orifice, as a greater proportion of the nozzle area is occupied by gas; as the droplet size produced is proportional to the square root of the liquid film thickness in the exit orifice (Lefebvre, 1988b), the droplet SMD decreases. An increased ALR also increases the volumetric expansion within the emerging two-phase flow, therefore the

droplet velocity increases (Jobehdar, 2014; Huang et al., 2008; Jedelsky et al., 2008; Panchagnula and Sojka, 1999) and the spray cone half-angle widens (Sovani et al., 2001; Jagannathan et al., 2011; Chen et al., 1994; Whitlow and Lefebvre, 1993; Wade et al., 1999).

Next, a brief review of past studies that have considered operating pressure, aerator design, and mixing chamber designs in determining their effect on the effervescent atomizer performance is provided. The operating pressure is controlled by varying the injection pressure of either fluids and is a common independent variable within effervescent atomizer studies. The distribution of investigated operating pressures within the literature demonstrates that effervescent atomizers are typically operated at much lower pressures than alternative techniques. The median value of the reports surveyed is just 5 bar, which compares to an arbitrary pressure swirl atomizer for direct gasoline injection at 50 bar (Vanderwege and Hochgreb, 1998). There are, however, some effervescent atomizer studies conducted at comparably high operating pressures; for example, Sovani et al. (2001) at 365 bar_g and Sovani et al. (2005) at 289 bar_g. The effect of increasing the operating pressure has been shown to positively affect both the internal flow and atomization performance of an effervescent atomizer (Lefebvre, 1996; Sovani et al., 2001b; Lefebvre et al., 1988), although some researchers report this effect is minor compared to the ALR (Jedelsky et al., 2009; Petersen et al., 2001).

Increasing the operating pressure has been shown to have a favorable effect on the internal flow for effervescent atomization. First, a greater operating pressure acts to increase the liquid mass flow rate through the atomizer, which promotes bubbling at the aerator due to an increased liquid cross-flow velocity and turbulent bubble breakup in the mixing chamber (Lefebvre, 1988b). In addition, greater operating pressures compress the gas phase, which results in a decreased bubble size (Rahman et al., 2012), with a reduced chance of collision and hence suppressed coalescence (Yang et al., 2007). Consequently, the range of ALRs over which bubbly flow can be maintained is increased with greater operating pressures (Chin and Lefebvre, 1993). Increasing the operating pressure also promotes improved atomization due to greater two-phase atomization intensity (Sojka and Lefebvre, 1990). This is generally reported to result in decreased droplet size (Lefebvre, 1988b; Sojka and Lefebvre, 1990; Konstantinov, 2012; Jedelsky et al., 2009; Petersen et al., 2001; Huang et al., 2008; Wang et al., 1989; Schröder et al., 2011; Whitlow and Lefebvre, 1993; Lefebvre et al., 1988; Huang et al., 2011; Wade et al., 1999; Chen et al., 1993), increased droplet velocity (Jedelsky et al., 2008; Panchagnula and Sojka, 1999), and increased spray cone angle (Sovani et al., 2001; Chen et al., 1994; Whitlow and Lefebvre, 1993; Wade et al., 1999). However, some researchers report that operating pressure has an insignificant effect, particularly for high viscosity liquids (Buckner and Sojka, 1991; Geckler and Sojka, 2008) and certain ALRs thought to correspond to the annular flow regime; for example, $>$ 20% ALR (Sojka and Lefebvre, 1990) and $>$ 15% ALR (Sojka et al., 1993).

Next, a discussion of past studies concerning aerator designs is provided. There are many elements of aerator design (e.g., atomizer configuration, aeration area, orifice diameter) that could affect the internal flow and subsequent atomization performance, and therefore there have been many reports considering elements of aerator design as an independent variable. Aerator design is considered to have a relatively minor effect on effervescent atomizer performance in comparison to other parameters (e.g., ALR and operating pressure) (Jedelsky et al., 2009; Wang et al., 1989; Lefebvre et al., 1988), however its effects have been assessed only by identifying the flow regimes formed in the mixing chamber and by analyzing the spray quality—the effect of aerator design on the gas-injection processes at the aerator itself, and hence the link to the flow regimes has not been established in the effervescent atomizer literature.

The comparative merits between atomizer configurations are rarely studied, however it is reported that, due to a comparatively large liquid flow area, an outside-in configuration has a reduced tendency to clog (Jedelsky et al., 2009) and is therefore preferred for high flow rate applications over the inside-out configuration (Sovani et al., 2001b). A problem thought to exclusively affect inside-out configurations is the bluff body recirculation effects of the aerator body, which (as previously discussed in Part I) can result in the formation of a large gas void in the aerator wake (Jobedhar, 2014). It is thought, however, that bluff body recirculation can be mitigated by streamlining the aerator body to reduce the wake effect, hence improving internal flow performance. This is supported by Jobedhar (2014), who reported that gas void formation was prevented with installation of an arbitrary conical aerator tip, which resulted in increased bubbly flow homogeneity and hence improved spray stability.

It has been previously discussed that the gas velocity through the aerator orifice affects the bubbling regime at the aerator, where bubbly flow is encouraged by a low gas injection velocity; for a given gas flow rate, this is achieved by increasing the aeration area. A wide range of aeration areas are referenced within the literature, which is thought to reflect the vast array of different fluid flow rates investigated. The result of increasing the aeration area is underresearched within effervescent atomizer literature, with its effect on gas injection and internal flow unreported, and the resulting atomization quality disputed, with some researchers reporting decreased SMD (Jedelsky et al., 2009; Chin and Lefebvre, 1995), and others reporting an insignificant effect (Broniarz-Press et al., 2010; Petersen et al., 2001). In a separate study, Jedelsky et al. (2008) reported that an increase in aeration area acts to decrease the spray cone angle.

The mixing chamber is the region in which the two-phase flow regime is stabilized, with the objective of supplying the exit orifice with the desirable flow conditions. Relatively few researchers have investigated mixing chamber design as an independent variable, predominantly thought to be due to the difficulty of varying this aspect of design without significant modifications to the experimental rig. Conventional mixing chambers have cylindrical form, with some researchers utilizing rectangular designs to gain beneficial optical properties for internal flow studies (Sojka and Lefebvre, 1990; Catlin and Swithenbank, 2001; Jagannathan et al., 2011).

A wide range of mixing chamber diameters (2–30 mm) are referenced in the literature, which are shown to have weak correlation with the intended liquid flow rate; consequently, it can be concluded that there is little conformity on atomizer size among researchers. The effect of mixing chamber diameter on the internal flow has not been investigated; however, it is reported to have minor influence on the subsequent two-phase atomization (Buckner and Sojka, 1993), with Petersen et al. (2001) reporting it to have an insignificant effect on droplet SMD. Jedelsky et al. (2009), however, reported optimum performance with the mixing chamber diameter designed to be four times larger than the exit orifice. Consideration should be given to ensure that it is suitably small to prevent phase separation or gravitational effects to become dominant over the surface tension (i.e., conditions in which orientation does not affect atomization). Kim and Lee (2001) reported phase separation can be prevented by diameters less than 10 mm, although the majority of effervescent atomizer studies exceed this criterion.

A number of parameters other than the ones discussed above also affect the atomizer performance. For instance, exit orifice design, liquid properties, orientation of the atomizer, atomizing gas properties, among other parameters affect both internal flow and spray characteristics. As such, the factors reviewed earlier in this section do not form an exhaustive list of operating parameters affecting the internal flow field, but are factors important from the present work's point of view.

The previous paper (Part I) compared the internal flow of effervescent atomizer with conventional flat-end aerator body and four different streamlined aerator designs. The DARPA SUBOFF afterbody (ADARPA) design (which is common in the conventional ship designs) was shown to be the best streamline design for an aerator body to produce required bubbly internal flow and minimal bluff body effect. This paper reports detailed internal flow visualization and its dependence on operating parameters (i.e., ALR), operating pressure, aerator, and mixing chamber design parameters, which to the authors' best knowledge, has never been studied and reported before. The work described in both Parts I and II have been reported in the PhD thesis of Niland (2017). From here forward, the DARPA SUBOFF afterbody design is referred to as ADARPA in the subsequent discussion.

2. EXPERIMENTAL SETUP AND DIAGNOSTICS

We refer the reader to Part I of this two-part study, where the experimental facility employed is described in detail. The high-speed shadowgraphy, which is employed to study internal flow and the near-nozzle atomization process has also been described there. In addition to high-speed shadowgraphy, particle Doppler anemometer (PDA) has been employed in the current study, which is explained here.

PDA is an optical technique, using light scattering to quantify the number, size, and velocity of particles within a flow. It is a time-averaged point measurement technique, which is suited for detecting small particles in the range of 0.005–1.4 mm diameter (Laakkonen et al., 2006); hence, it is a commonly referenced spray characterization technique within effervescent atomizer studies. A major limitation of PDA is that it is not suitable for dense spray applications, whereby the intensity of measurement light decreases due to attenuation through the spray (Gomez, 2010).

Laser light is supplied to the DualPDA system via a Coherent Innova 70 multiline argon ion laser. The beam is first directed into a Dantec® 60 $\times$ 40 FiberFlow transmitter, which performs the function of splitting it into six beams of three wavelengths and applying a 40 MHz frequency shift with a Bragg cell to one beam of each color; consequently, two green (514.5 nm), two blue (488.0 nm), and two violet (476.5 nm) beams are produced. The current testing is configured in a 2D mode (i.e., detecting axial and radial velocities and droplet diameters), and therefore only the green and blue beams are supplied to the 112 mm fiber PDA transmitting optics, using Dantec® 60 $\times$ 24 manipulators to align the beams into the fiber optic delivery lines. The 1.5 mm diameter transmitted beams are separated by 74 mm at the optics, converging to form the measurement volume. Both transmitting and receiving optics are configured with 600 mm focal length lenses, which allow sufficient clearance from the spray to prevent wetting of the equipment. The receiving optics are angled 74° from forward scatter, which corresponds to the optimal angle for refracted scattered light for a water droplet in air (Dantec Dynamics User Guide, 2006), and configured with aperture plate C, which allows for measurement of droplets up to approximately 600 μm diameter. The particle burst signals are detected by photomultipliers within the receiving optics, which are transferred and managed by a Dantec® 58N10 PDA BSA processing unit before being sent to a computer for further processing, presentation, and storage by Dantec Dynamics® BSA flow software.

The optics are mounted onto a three-axis traverse, which allowed movement of the control volume within the spray, and was automatically controlled via a connected PC with Dantec® SIZEWARE software. A suitable traverse mesh should have sufficient measurement locations to provide data representative of the spray profile, but few enough points to minimize computational and time resources. An identical traverse mesh is used across the PDA experimentation and

hence the data collection is structured and consistent for all investigations. For each individual investigation, 285 individual measurement locations are examined, which corresponds to 1 mm radial spacing for 25, 50, 100, and 150 mm axial displacements, and 2 mm radial spacing for 200 and 250 mm axial displacements. Axisymmetry assumption is made, and resultantly, the measurements are made in only one half at a given axial section. A fixed five–second sampling duration for each measurement location is adopted.

3. TEST CASES AND EXPERIMENTAL CONDITIONS

In order to characterize the internal flow of effervescent atomizer with ADARPA streamlined aerator design and to study the effect of various independent parameters on the internal flow behavior, seven different ADARPA streamlined aerators (A1A–A7A) with different aerator holes configuration as shown in Fig. 1 are employed. The outer tube diameter of all aerators is 10 mm. The different aerator hole configurations are named $n \times \phi m$. Here, n represents the number of holes on the aerator surface of diameter m, which is in millimeters.

The effect of ALR on the internal flow is studied for each aerator (A1A–A7A). Various liquid flow rates employed are 30, 60, 90, 120, 180, 240, and 290 g/s. The corresponding liquid Baker parameter (the reader is referred to Part I of this paper for a detailed description of the Baker parameters) range is 95.5–923 kg/m^{2}s. Gauge pressure in the atomizer of 5 bar is maintained by

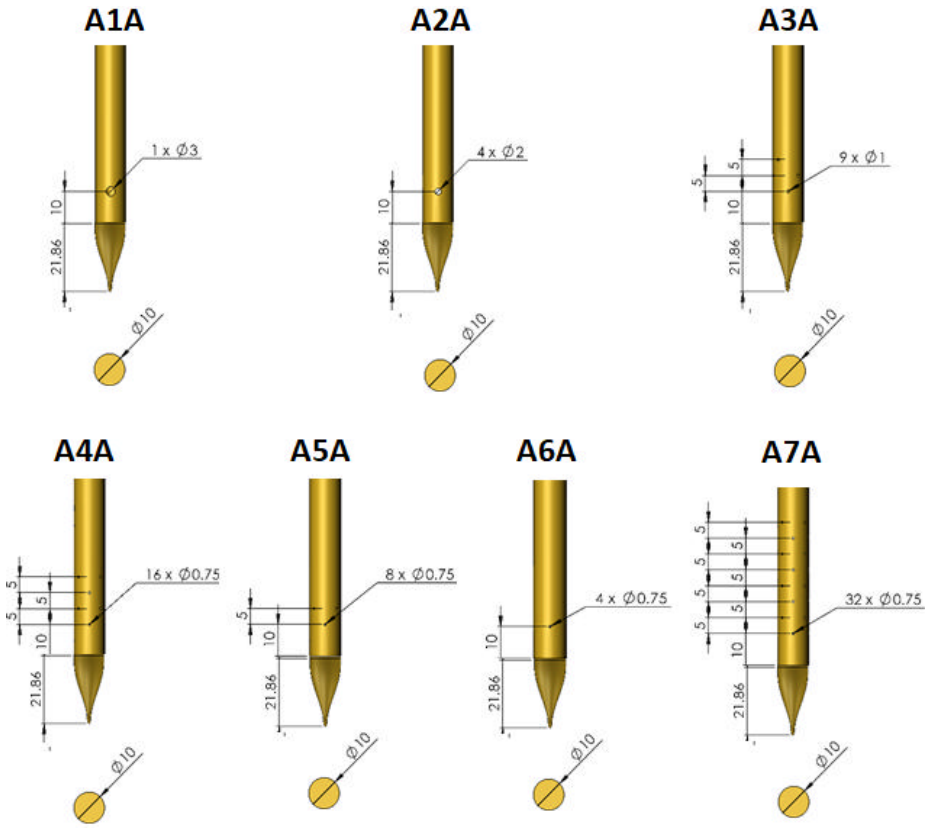

FIG. 1: Different ADARPA aerator body configurations employed in the present study

controlling the discharge valve setting (for internal flow visualization) for each of these liquid flows or by employing interchangeable exit orifices of different diameters (for characterizing the spray). For each liquid flow rate the gas supply (from 7 bar compressed air line) is varied in increments to achieve ALR of 0.12, 0.25, 0.5, 1.0, 1.5, 2.0, 3.0, 4.0, and 5.0%. The stabilized two-phase internal flow at each of these ALRs for every aerator is imaged using high-speed shadowgraphy. Each test is repeated three times to determine repeatability.

In order to study the effect of aerator orifice diameter on the internal flow the aerator configurations A1A, A2A, A3A, and A6A are considered (Table 1). Each of these aerators has an outer tube diameter of 10 mm, an ADARPA streamlined body, and common aeration area of 7.07 mm^2. To maintain a common aeration area with differing aerator orifice diameters, the aeration orifice configuration (e.g., number of orifices, hole positioning) is required to be varied between the investigated aerators—in general, the intention of the aerator designs is to maximize the orifice spacing within a 15 mm region and 10 mm from the aerator tip.

Aeration area is investigated as an independent variable by considering aerator configurations A4A (combined area of aeration holes: 1.77 mm^2), A5A (area: 3,53 mm^2), A6A (area: 7.07 mm^2), and A7A (area: 14.14 mm^2) as shown in Table 1. Each of these aerators has an aerator orifice diameter of 0.75 mm, an outer tube diameter of 10 mm, and a streamlined ADARPA body. The other independent parameters considered in the present study are mixing chamber diameter and operating pressure. These are investigated with aerator configuration A6A as depicted in Table 1.

4. RESULTS

4.1 Effect of ALR on the Internal Flow of an ADARPA Atomizer

It is observed that there is a significant effect of ALR on the internal flow and near-nozzle spray characteristics of an effervescent atomizer equipped with an ADARPA streamlined aerator tip. The internal flow is composed of (1) gas injection at the aerator orifice into the mixing chamber and (2) stabilized two-phase gas-liquid flow regime in the mixing chamber. The dependence of a gas injection mechanism at the aerator orifice into the mixing chamber and the resultant spray characteristics at the nozzle exit on ALR is discussed here.

TABLE 1: ADARPA atomizer configurations and flow settings employed to study the effect of various independent parameters on the internal flow

Experimental parameter	Aerator orifice diameter comparison	Aerator area comparison	Mixing chamber diameter comparison	Operating pressure comparison
Discharge valve setting (g/s)	30–290	30–290	30–290	30–225 30–130
ALR (%)	0–5	0–5	0–5	0–5
Aerator geometry	A1A, A2A, A3A, A6A	A4A, A5A, A6A, A7A	A6A	A6A
Mixing chamber diameter (mm)	20	20	14, 20, 25	20
Operating pressure (bar)	5	5	5	1, 3, 5

4.1.1 Effect of ALR on the Gas Injection Mechanism

Figure 2 depicts the dependence of a gas-injection mechanism on ALR for the aerator geometry A6A (shown in Fig. 1). The gas-injection mechanisms for other geometries are either the same or a subset of the mechanisms discussed for this aerator, and as such, the design A6A can be considered to represent a generic case. The results are comparable with all other ADARPA aerator configurations presented within this work.

The process of gas injection is observed at the aerator orifice exit (regions marked in Fig. 2) and quantified for the first time for the ADARPA aerator tip atomizer by categorizing each observation into common regimes. This is performed across various fluid flow rates, which resulted in the identification of five different gas injection regimes. These are a combination of the standard gas injection regimes defined previously in the literature, and a new regime defined in the current work to better describe the experimental observations. Each of these is discussed as follows.

4.1.1.1 Single Bubbling

Single bubbling is observed to be the formation of individual uniformly sized bubbles, which are either sheared directly from the emerging gas phase at the aerator orifice or detached from a short teardrop-shaped gas neck within the peripheral liquid flow [Fig. 2(a)]; this is in agreement with literature descriptions (Loubière et al., 2004; Forrester et al., 1998; Balzán et al., 2017). Upon injection, the bubbles are drawn away from the aerator with the liquid flow into the mixing chamber.

The formation of a single bubble can be explained as follows. In general, the stability of the emerging gas phase, and hence its resistance to break up into bubbles, is seen to decrease with:

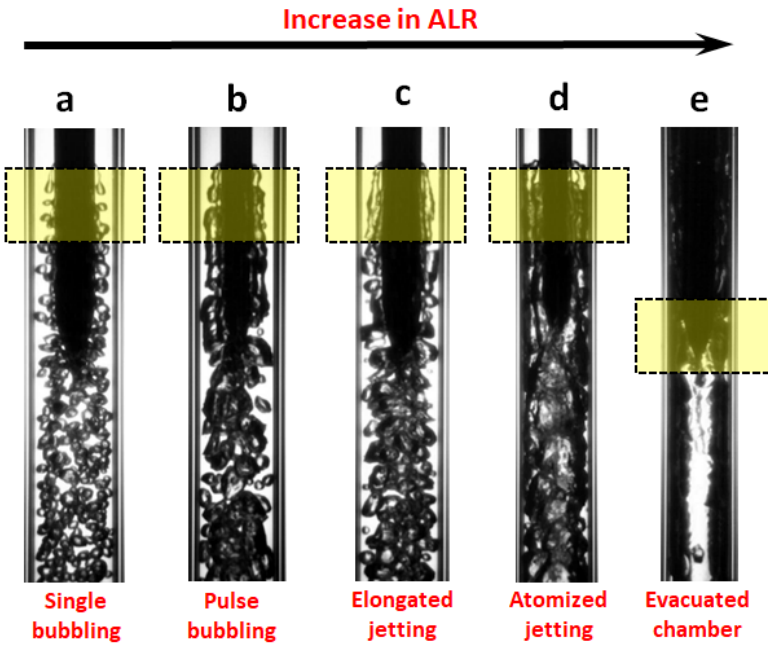

FIG. 2: Representative images depicting the effect of ALR on gas injection mechanism for the aerator geometry A6A: (a) 0.185% ALR; (b) 0.48% ALR; (c) 1.5% ALR; (d) 2.04% ALR; (e) 4.5% ALR

- High relative detachment forces: these forces are generated by strong detachment mechanisms, for example, viscous forces generated by high liquid cross-flow velocity (e.g., drag, inertia); and weak restoring mechanisms, for example, buoyancy. High detachment forces are encouraged by high liquid flow rates (e.g., large exit orifice diameters, increased operating pressure), small mixing chamber diameters, and vertically upward orientation.
- High emerging gas-liquid interface area: this increases the exposed area of the emerging gas-phase over which the detachment mechanisms act. Small aerator orifice diameters encourage high gas-liquid interface areas.
- Low injected gas velocity: this increases the detachment rate of gas within the liquid cross-flow compared to the supply rate, which acts to suppress the generation of long gas necks connecting an otherwise detached bubble to the aerator orifice. Low injected gas velocity is a result of low gas-flow rates (i.e., low ALRs) and high aeration areas. Single bubbling is observed to be promoted by the injection of a highly unstable gas phase into a liquid continuum (i.e., highest relative detachment forces, highest emerging gas-liquid interface area, and/or lowest injected gas velocity), and hence was promoted by low ALRs. The region of single bubbling is depicted in Fig. 3, which shows different gas-phase injection regimes in the parameter space of operating liquid and gas Baker parameters. The corresponding liquid and gas flow rates are also shown.

4.1.1.2 Pulse Bubbling

Pulse bubbling [Fig. 2(b)] is observed for conditions in which the emerging gas phase has increased stability over single bubbling (i.e., increased ALR); thus, gas-phase injection generates

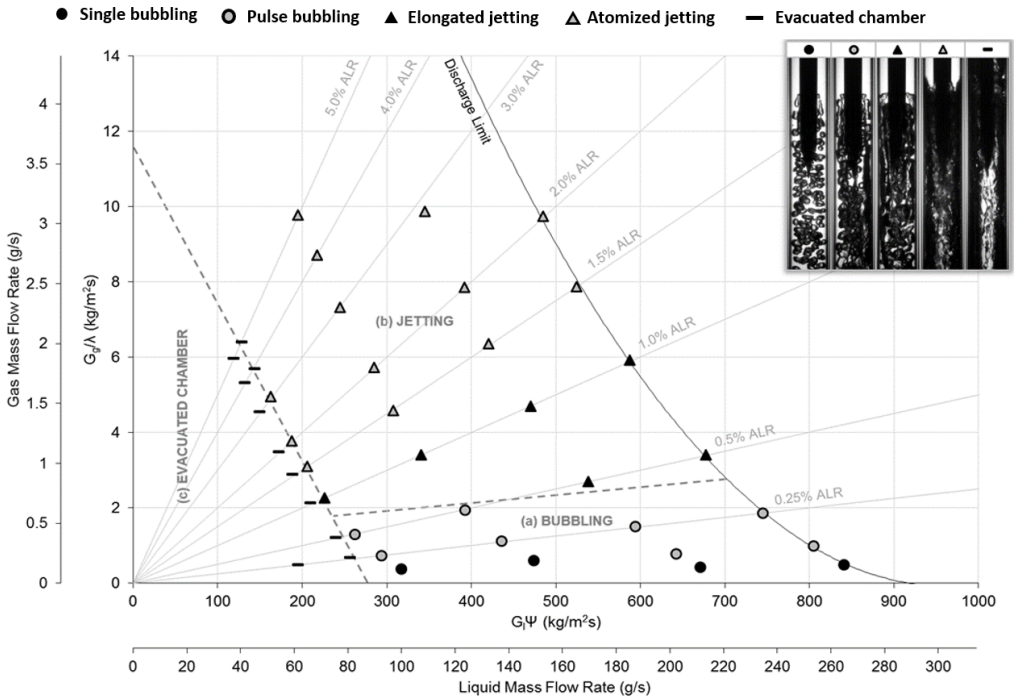

FIG. 3: Gas injection regime map for the aerator configuration A6A

gas entities of varying size (e.g., bubble and slugs). In the majority of pulse bubbling cases, a rippling gas neck is observed to be injected into the peripheral liquid flow, which resembles a series of interconnected gas entities. Given sufficient residence time and breakup mechanisms, these instabilities on the gas-liquid interface eventually gain sufficient amplitude to separate the neck into gas entities of varying size. The observations corresponding to pulse bubbling are in line with the definitions provided within the literature (Forrester et al., 1998; Balzán et al., 2017; Rigby et al., 1995). The region of pulse bubbling is shown in the regime map (Fig. 3), where the combined region of single and pulse bubbling is denoted as the bubbling regime.

4.1.1.3 Elongated Jetting

The elongated jetting regime is observed with increased stability of the emerging gas phase (e.g., increased ALR), where a continuous gas jet is injected from the aerator orifice, which can chaotically break up significantly downstream of the aerator; this is in agreement with the description recently proposed by Balzán et al. (2017). Increasing the ALR through the elongated regime causes the gas jet to emerge from the aerator orifice with ever-increasing momentum; this can cause it to contact with the mixing chamber, although little churning occurs. Infrequently, a small bubble may be generated due to exposure of the emerging jet to the liquid cross-flow, contact with the mixing chamber wall, or shearing of the gas-liquid interface, but this is not considered a suitable bubble formation mechanism for effervescent atomization. Examples of elongated jetting across a variety of experiments are shown in Fig. 2(c) and marked in the regime map in Fig. 3.

4.1.1.4 Atomized Jetting

Atomized jetting is promoted by a very stable emerging gas phase, in which a continuous gas jet is observed to be injected into the mixing chamber. This has visibly more chaos than that associated with elongated jetting and is in agreement with the descriptions recently proposed by Balzán et al. (2017). As the ALR increases within the atomizer jetting regime, the emerging gas jet becomes ever more turbulent with the majority of cases having sufficient momentum to contact the mixing chamber wall, often with significant churning. In addition, a small number of comparatively small bubbles were frequently sheared from the gas jet upon initial exposure of the gas phase to the liquid cross-flow, contact with the mixing chamber wall, or shearing of the gas-liquid interface; this is not considered a suitable bubble formation mechanism for effervescent atomization. Examples of atomized jetting across a variety of experiments are shown in Fig. 2(d) and marked in the regime map in Fig. 3, where the combined region of elongated jetting and atomized jetting is denoted as the jetting regime.

4.1.1.5 Evacuated Chamber

The evacuated chamber gas injection regime is first presented in the current work to describe a condition in which phase separation is achieved immediately upon liquid injection into the atomizer, resulting in a continuous gaseous core throughout the atomizer into which the gas is directly injected at the aerator. Every observed case of evacuated chamber occurred at critically low liquid flow rates, whereby the liquid drag and momentum upon startup is insufficient to displace the ambient air within the mixing chamber; hence passive bleeding of the atomizer is not achieved. Examples of evacuated chamber across a variety of experiments are shown in Fig. 2(e) and marked in the regime map in Fig. 3.

4.1.2 Effect of ALR on the Stabilized Gas-Liquid Flow Regime in the Mixing Chamber

Figure 4 depicts the dependence of mixing chamber gas-liquid phase flow on ALR for the aerator geometry A6A. The two-phase gas-liquid flow inside the mixing chamber is observed (in the regions marked in Fig. 4) and quantified for the first time for the ADARPA aerator tip atomizer by categorizing flow regime into six different categories. These are a combination of the standard flow regimes defined previously in the literature and new regimes defined in the current work to better describe the experimental observations. Each of these is discussed as follows.

4.1.2.1 Bubbly Flow

A bubbly flow [Fig. 4(a)] matching literature descriptions (Jobedhar, 2014; Furukawa and Fukano, 2001; Zhou, 2013; Usui and Sato, 1989; Bhagwat, 2011) is observed to be a homogenous two-phase flow consisting of uniformly sized bubbles within a liquid continuum that are produced at the aerator and flow unobstructed into the mixing chamber. However, not all bubbling cases at the aerator are observed to form consistent-sized bubbles; for example, pulse bubbling at relatively high ALRs is commonly observed to inject gas entities of variable sizes (i.e., bubbles and slugs) into the liquid cross-flow. Consequently, bubbly flow is encouraged by the injection of an unstable gas-phase, which is prone to rapid breakup upon exposure to the liquid cross-flow; this is promoted by low ALRs. Therefore, bubbly flow corresponds with the majority of single

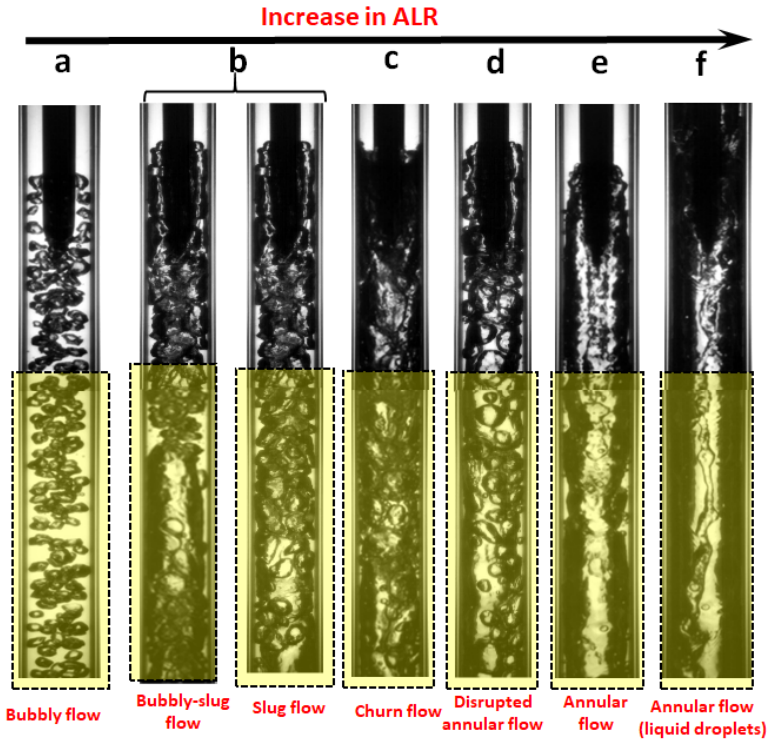

FIG. 4: Representative images depicting the effect of ALR on two-phase mixing chamber flow regime for the aerator geometry A6A: (a) 0.135% ALR; (b) 0.5% ALR; (c) 1.75% ALR; (d) 1.85% ALR; (e) 1.9% ALR; (f) 4.5% ALR

bubbling cases and low ALR cases of pulse bubbling. The regime of bubbly flow is shown in Fig. 5.

4.1.2.2 Slug Flow

Slug flow [Fig. 4(b)] is defined as the intermittent presence of large gas entities within a liquid continuum that have diameters similar to the mixing chamber; this is a standard flow regime referenced within the literature (Jobedhar, 2014; Furukawa and Fukano, 2001; Zhou, 2013; Usui and Sato, 1989; Bhagwat, 2011). The formation of a slug flow has been identified previously owing to (1) surface instabilities during co-flow gas injection (Yang et al., 2007; Cheung et al., 2012), (2) coalescence of bubbles within the mixing chamber (Yang et al., 2007; Liao et al., 2010; Tse et al., 1998; Laakkonen et al., 2006; Shinnar and Church, 1960; Cheung et al., 2012), (3) direct injection of gas slugs (Sen et al., 2014), and (4) breakup of gas jets into nonuniformly sized bubbles (Forrester et al., 1998). Accordingly, in the present study, slug flow was observed (Fig. 5) when gas injection is of type pulse bubbling, elongated jetting, and in some cases, atomized jetting (compare Figs. 3 and 5). In the ALR range up to $\sim$ 1.00% a bubbly-slug flow is also observed [Fig. 4(b)] wherein the slug region is identified in the flow; however, toward the end of the nozzle exit, the homogeneous bubbly flow prevails.

4.1.2.3 Churn Flow

Churn flow [Fig. 4(c)] is a chaotic two-phase flow in which neither phase is continuous. Every instance of churn flow within the current investigation coincided with jetting at the aerator, which

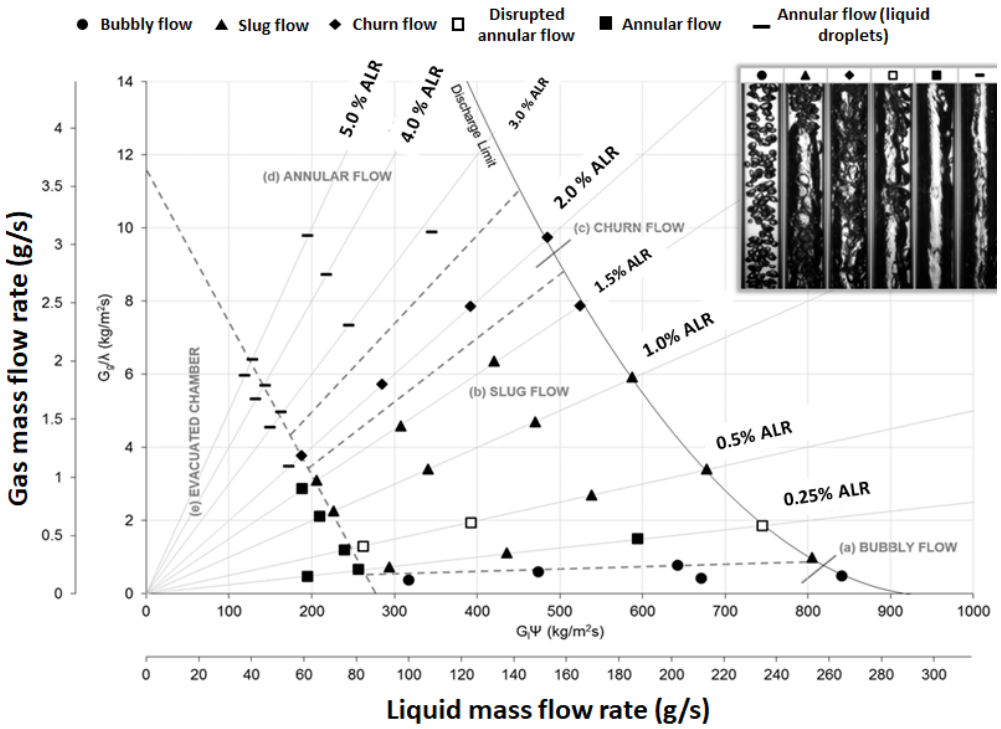

FIG. 5: Mixing chamber flow regime map for the aerator configuration A6A

mixes within the mixing chamber to form a chaotic heterogeneous regime. The regime of churn flow is shown in Fig. 5.

4.1.2.4 Disrupted Annular Flow

Disrupted annular flow [Fig. 4(d)] is first defined in the current work to describe observations of an otherwise constant gaseous core that is regularly separated by liquid ligaments; therefore, neither fluid phase is completely continuous. It is observed under conditions of high relative buoyancy due to the incomplete action of either coalescence or breakup. To elaborate, the formation of disrupted annular flow is encouraged by incomplete coalescence: disrupted annular flow is generally observed at a low liquid Baker parameter, just in excess of the evacuated chamber. This corresponds to conditions at which the relative effects of buoyancy are great enough to promote coalescence of the gas phase and thus prevent the formation of the standard intermittent flow regimes (i.e., slug flow, churn flow); however, the residence is too low to enable complete coalescence into an annular flow. Consequently, residual liquid ligaments remain across the otherwise constant gas core. Disrupted annular flow is also encouraged by incomplete breakup: in unusual cases, liquid ligaments are observed to be generated across a gas core due to the incomplete breakup of the gas phase, which is observed due to gas-liquid interface surface instabilities and the interference of gas entities within the peripheral liquid flow, without separation being achieved.

4.1.2.5 Annular Flow

Annular flow [Fig. 4(e)] is widely cited within the internal flow literature (Jobedhar, 2014; Furukawa and Fukano, 2001; Zhou, 2013; Usui and Sato, 1989; Bhagwat, 2011) to be a continuous gaseous core formed in the center of the mixing chamber surrounded by a peripheral liquid flow. Any surface instabilities generated on the gas-liquid interface or gas entities within the liquid periphery are not great enough to generate breakup of the gas core within the length of the mixing chamber, which results in annular flow.

4.1.2.6 Annular Flow (Liquid Droplets)

Annular flow (liquid droplets) shown in Fig. 4(f) is a unique flow regime observed in the current experimentation. It is defined by a relatively constant annular core, which encloses liquid droplets generated by dripping from the central aerator tube. The liquid droplets are occasionally seen to interfere with the liquid periphery, which can form liquid ligaments spanning the mixing chamber (akin to disrupted annular flow or churn flow). Annular flow (liquid droplets) has a tendency to occur at high liquid flow rates and ALRs, where annular flow would otherwise be expected, although there are some isolated exceptions to this rule. It is not observed for vertically upward orientation (images not shown here for brevity) as the liquid droplets are formed under the action of gravity. This flow regime is not thought to apply to outside-in effervescent atomizers, as the central aerator tube from which the liquid drips would not be present.

Annular flow (liquid droplets) is not equivalent to a “wispy annular flow,” which is occasionally cited in the literature. Wispy annular flow also features liquid droplets within a gaseous core, but these are small droplets generated due to the inner phase shearing, not large liquid droplets from dripping at the aerator. The regimes of annular flow consisting of disrupted annular flow, annular flow, and annular flow (liquid droplets) are shown in Fig. 5.

It is observed in the present experimental study that the internal flow field is also significantly influenced by (1) aerator orifice diameter, (2) aeration area, (3) mixing chamber diameter, and (4) operating pressure. This list presents the independent parameters considered in the present study and is by no means an exhaustive one. The effect of each of these parameters on the internal flow will be discussed in the next four subsections.

4.1.3 Effect of ALR on the Spray Characteristics

While it is important to understand the effect of ALR on internal flow as described in the previous two subsections, it is equally important to understand its effect on spray characteristics. For this purpose, near-nozzle shadowgraphy and PDA have been employed in the present study. The spray characterization, however, was possible only for bubbly, bubbly-slug, slug, and some part of churn flow regimes (i.e., for ALR range $\sim$ 0–1.5% ALR). This is because the spray generated in flow cases at ALRs in excess of $\sim$ 2.0% was too unstable. However, the range of ALR amenable to PDA still depicts some interesting features that are discussed here.

Figure 6 depicts the near-nozzle spray characteristics and droplet size and velocities as ALR is varied. Particle size distribution is presented in unweighted (D10) form [i.e., arithmetic mean diameter (AMD)]. This is because only $\sim$ 52% confidence limit was achieved for weighted average data (i.e., D32, SMD) particularly for poorly atomized sprays on the spray edge within the chosen 5 s sampling duration, whereas a confidence limit of $\sim$ 95% is usually preferred. To achieve a $\sim$ 95% confidence limit in the acquisition position within the spray volume (i.e., 2D analysis, as in the present case), a very high sampling duration was determined to be necessary ($\sim$ 150–200 s) at each of 285 measurement locations. Thus, it was considered impractical, and data are presented in unweighted form. Although this is a limitation of the present study, it still enables identification of flow features and related spray properties. The spray edge (Fig. 6) is defined as the radial position at which data rates dropped below 10% of their maximum at that axial location. The gas velocity is determined by assuming that droplets with diameter less than 2 μm act as seeding particles within the gas flow. For locations that have no droplets satisfying this criterion, the gas velocity cannot be determined and, hence, is assumed to be zero. It is observed from Fig. 6(a) that the internal flow at the lowest ALR (0.12% ALR) is seen to be a bubbly flow, with a low number of small bubbles existing in the liquid continuum. Consequently, the single bubble atomization is relatively irregular and hence the spray quality is poor, with a large quantity of unatomized liquid ligaments in the spray centerline. A high number of large droplets ($\sim$ 150–180 μm: D10) exist in the centerline at the lowest ALR (0.12% ALR), which corresponds to the observations of a sparse bubbly flow and hence poorly atomized liquid ligaments. The associated velocities are $\sim$ 35 m/s in the near nozzle region of $\sim$ 200 mm from the nozzle exit. As the ALR is increased from 0.12% to 0.25% and thereafter until $\sim$ 1.00% [Figs. 6(b)–6(d)], internal flow regime resulted in a bubbly and bubbly-slug flow with a greater number density of small bubbles. This provided greater homogeneity, hence the regularity of the single bubble atomization increased, which generated a more consistent and stable spray. Raising the ALR acts to increase the average gas velocity (up to $\sim$ 50 m/s) within the spray, particularly in the near-nozzle region as the gas expands from the exit orifice. Consequently, greater destructive mechanisms are exerted on the liquid phase with increasing ALR, and hence finer atomization is achieved ($\sim$ 40–50 μm). Furthermore, the largest droplets ($\sim$ 70–80 μm) are seen to migrate to the spray edge as the ALR increases, as the droplet momentum due to the expanding gas carries the larger droplets away from the nozzle axis. This is in keeping with literature reports (Jedelsky et al., 2003; Liu et al., 2011; Gomez, 2010; Jedelsky and Jícha, 2016).

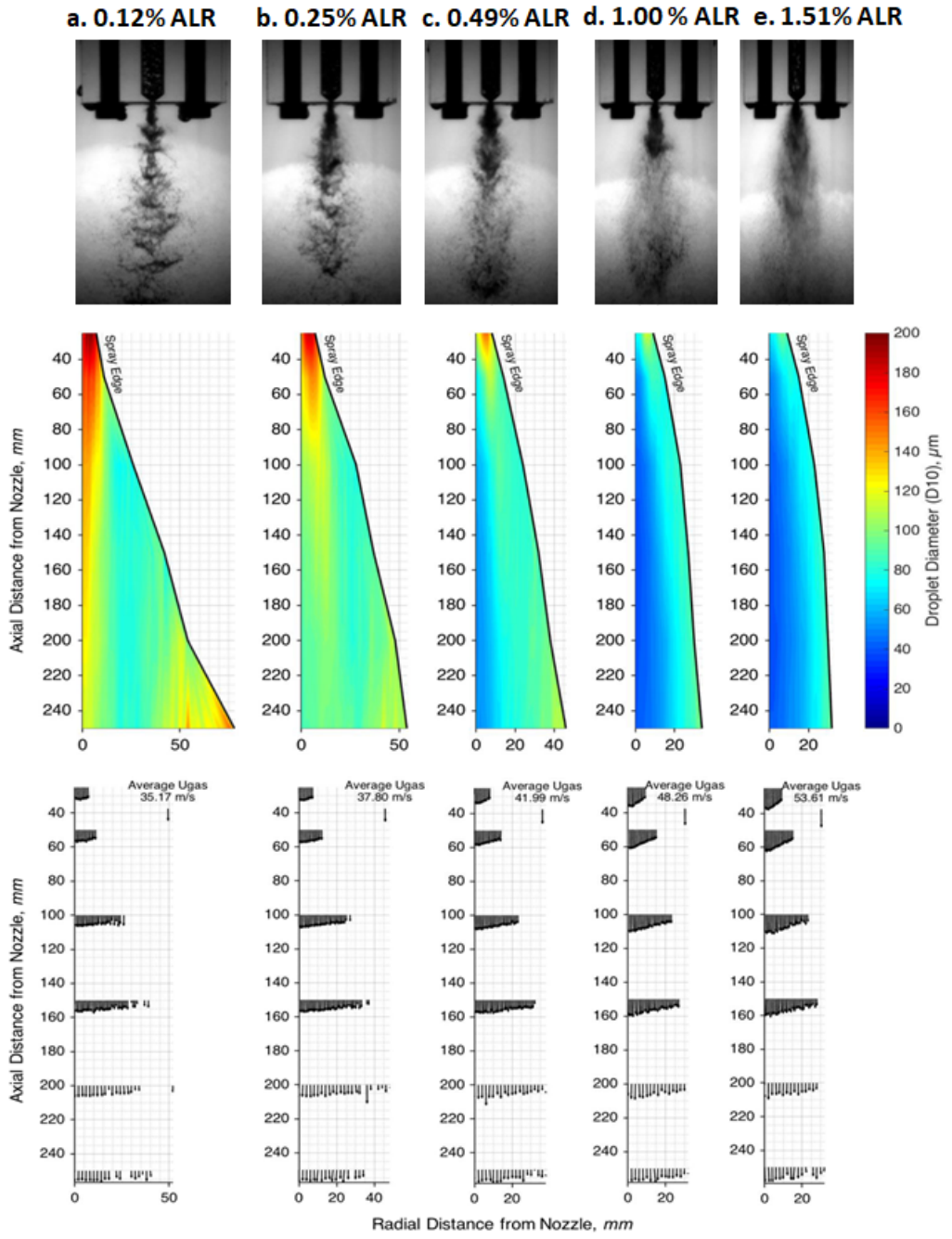

FIG. 6: Near nozzle atomization (top row), droplet spray size profiles (middle row), and gas velocity quiver plot (bottom row) for (a) 0.12% ALR; (b) 0.25% ALR; (c) 0.49% ALR; (d) 1.00% ALR; (e) 1.51% ALR

In addition, droplets sizes are seen to decrease with axial distance, which is thought to be due to the action of secondary atomization, as droplets break up within the ambient atmosphere. The

spray characteristics at $\sim$ 1.5% ALR shown in Fig. 6(e) are evidenced when the flow regime is bubbly-slug flow [slug flow present in the flow region but the homogeneous bubbly flow prevailing toward the end of nozzle exit as shown in Fig. 4(b)]. However, consistent and stable spray with favorable single bubble atomization is predominantly observed within 1.00% ALR. This is also the case witnessed in further subsections of this study, where different operating parameters with different aerator configurations are employed. In most of the cases a consistent high-density bubbly and bubbly-slug flow are witnessed within 1.00% ALR operating range.

4.2 Effect of Aerator Orifice Diameter

The effect of aerator orifice diameter is studied by considering aerator configurations A1A, A2A, A3A, and A6A. The diameter is varied between 0.75 (A6A) and 3.0 (A1A) mm for a common aeration area of 7.07 mm^2. The injected bubble size in the interior of the effervescent atomizer is known to be proportional to the aerator orifice diameter, and therefore a reduction in aerator orifice diameter is expected to reduce the bubble size for a given ALR, and hence, to increase flow homogeneity.

Figure 7(i) shows the effect of varying the aerator orifice diameter at common 0.12% ALR and with a fully open discharge nozzle. Reducing the aerator orifice diameter (from A1A to A2A to A3A to A6A) is observed to reduce to stability of the emerging gas phase, therefore promoting the detachment of bubbles. For the largest aerator orifice diameter investigated (A1A), the emerging gas phase is relatively stable, and therefore a gas jet is formed, which irregularly detaches from the orifice to form a very large gas slug. This compares to the reduced aerator diameters [A2A, A3A, and A6A; Fig. 7(i)], in which the gas phase is observed breaking up into bubbles upon exposure to the liquid cross-flow and forming a bubbly flow in the mixing chamber. Due to the increasingly premature detachment of the gas phase, the bubble size is visibly observed to reduce with decreasing aerator orifice diameter.

The purpose of an effervescent atomizer aerator is to inject the gas phase into the liquid phase to form uniformly sized bubbles and, hence, generate a homogenous and dense bubbly flow resulting in favorable spray characteristics. Therefore, a region in the parameter space of gas mass flow rate (ordinate) and liquid mass flow rate (abscissa) can be drawn, representing all flow setting combinations (gas and liquid mass flow rates) that produce desired dense bubbly and bubbly-slug flow regimes. These regions for the aerators discussed in this subsection are shown in Fig. 7(ii). For all of these cases, the bubbling region was restricted at (a) high ALRs, by the transition to jetting regimes. Decreasing the aerator orifice diameter increases the ALR at which bubbling transitions to jetting, as a result of a less stable emerging gas phase; this is thought to be caused by an increased emerging gas-liquid interface area over which the detachment mechanisms act. (b) Low liquid flow rates, by the generation of evacuated chamber. While this limit was observed to marginally vary between aerator orifice diameters, the trend was not predictable. It is thought that the differences are due to the chaotic mechanisms affecting passive bleeding of the atomizer upon startup and not the effect of the aerator orifice diameter. (c) High liquid flow rates, by the flow limit of the discharge valve. Increasing the ALR acts to further restrict the valve, hence the liquid flow rate continually decreases. The effect of aerator orifice diameter was not seen to have a significant effect on the discharge limit.

The OR_{bubbling} (defined in Part I of this two-part series) for the four aerators (A1A, A2A, A3A, and A6A) discussed in the present subsection are shown in Fig. 7(iii) as specific points marked with crossmarks. It is observed that OR_{bubbling} increases with a decrease in aerator orifice diameter. Further, in order to determine OR_{bubbling} at intermediate aerator diameters within the

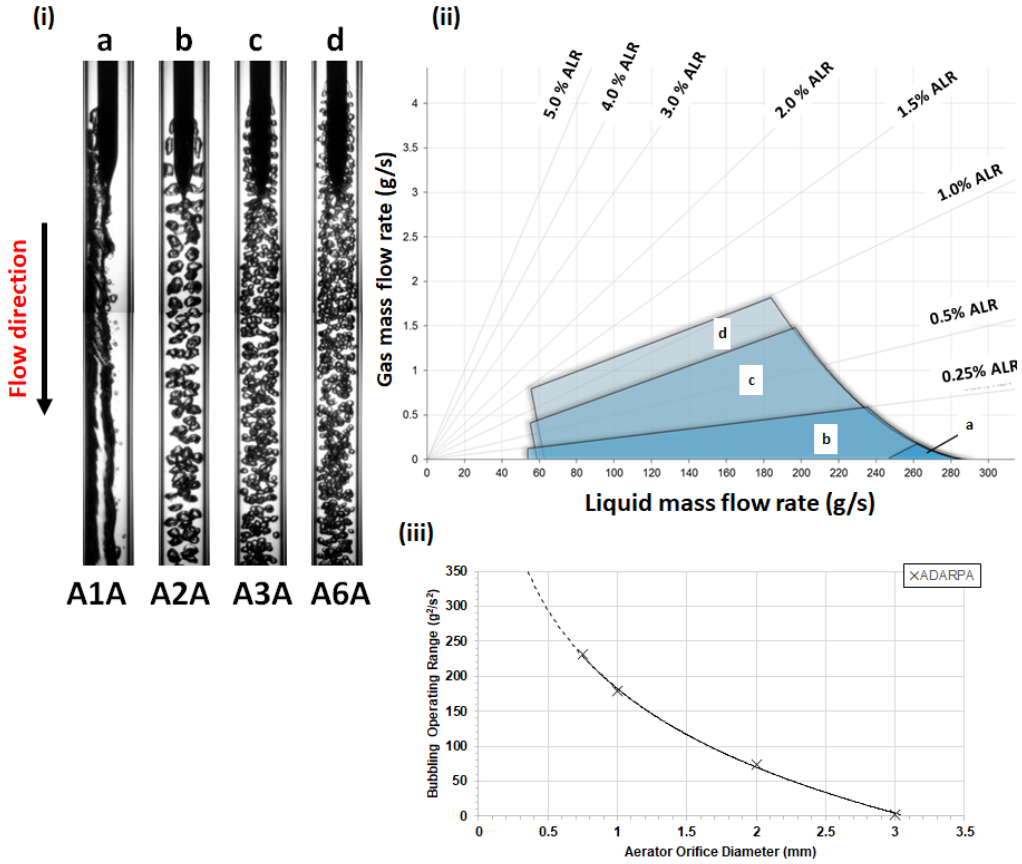

FIG. 7: (i) Comparable observations with varying aerator orifice diameter: (a) Aerator A1A – 1 × 3.0 mm, flow rate: 252 g/s, 0.12% ALR; (b) Aerator A2A – 4 × 2.0 mm, 252 g/s, 0.12% ALR; (c) Aerator A3A – 9 × 1.0 mm, 252 g/s, 0.12% ALR; (d) Aerator A6A – 16 × 0.75 mm, 251 g/s, 0.12% ALR. Liquid Baker parameter for all four cases is approximately 802.54 kg/m^{2}s. (ii) Effect of aerator orifice diameter on bubbling operating range: (a) aerator A1A; (b) aerator A2A; (c) aerator A3A; (d) aerator A6A. (iii) Dependence of aerator orifice diameter on bubbling operating range.

range employed in A1A–A6A—different from the diameters employed in A1A, A2A, A3A, and A6A—a curve is fit for the crossmarks and is represented by a solid line in Fig. 7(iii). This curve can be useful for designers or modelers to determine the OR_{bubbling} in the aerator orifice diameter range considered in the present study. The spray characteristics of bubbly and bubbly-slug flows are expected to be similar to those previously described in the previous subsection and as such are not reported here.

4.3 Effect of Aeration Area

In this subsection, the dependence of aeration area on the internal flow of effervescent atomizers is discussed. To consider this effect, a study of the internal flow of four different aerator configurations (i.e., A4A–A7A, as previously shown in Fig. 1) is accomplished. The effect of aerator aeration area on effervescent atomizer internal flow is investigated between 1.77 mm^2 (A4A)

and 14.14 mm^2 (A7A) with an ADARPA aerator body design. In order to maintain continuity, increasing the aeration area acts to decrease the injected gas velocity. In the current investigation, the aeration area is varied for the same aerator orifice diameter by increasing the number of holes.

Figure 8(i) shows the effect of aeration area on the internal flow of an effervescent atomizer at a comparable ALR and exit orifice diameter (i.e., discharge nozzle set to fully open). At the lowest aeration area, the injected gas velocity is highest and, hence, the rate of gas supply to the emerging gas phase is high compared to the detachment rate within the liquid cross-flow. This promotes formation of gas jets from the orifices, which intermittently detach from the orifice in a pulse bubbling regime to form a slug flow. However, the effect of increasing the aeration area decreases the injected gas velocity, and hence is seen to reduce the length of the gas neck from which bubbles are formed; therefore, the rate of detachment increases and single bubbling and bubbly flow are promoted.

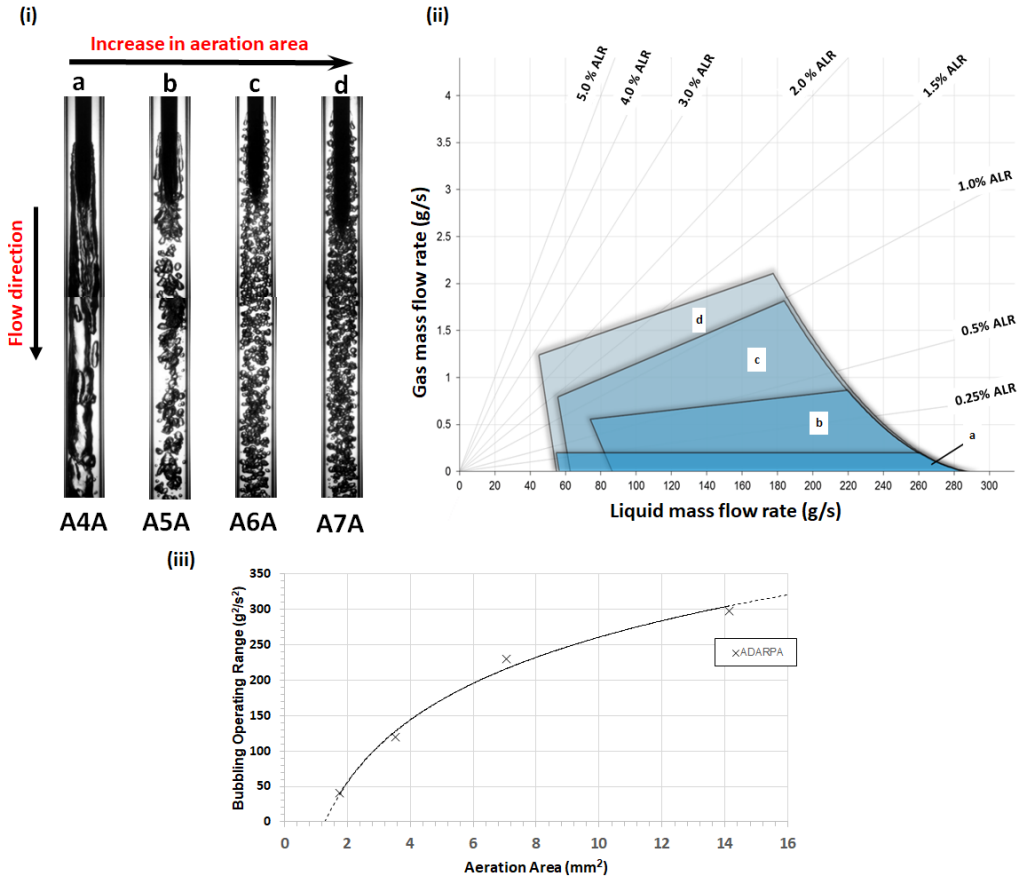

FIG. 8: (i) Comparable observations of varying aeration area: (a) Aerator A4A – 1.77 mm^2, 253 g/s, 0.12% ALR; (b) Aerator A5A – 3.53 mm^2, 253 g/s, 0.12% ALR; (c) Aerator A6A – 7.07 mm^2, 251 g/s, 0.12% ALR; (d) Aerator A7A – 14.14 mm^2, 252 g/s, 0.12% ALR. Liquid Baker parameter for all four cases is approximately 802.54 kg/m^{2}s. (ii) Effect of aerator area on bubbling operating range: (a) aerator A4A; (b) aerator A5A; (c) aerator A6A; (d) aerator A7A. (iii) Dependence of aerator area on bubbling operating range.

ALR range within which bubbly flow is produced for each of these aerators is shown in Fig. 8(ii). The bubbling regions for all cases are limited at (a) high ALRs, by the transition to jetting regimes. Decreasing the aeration area increased the ALR, at which bubbling transitions to jetting, indicating a less stable emerging gas phase thought to be caused by a reduced injected gas velocity, which increases the detachment rate of gas compared to the supply rate. (b) Low liquid flow rates, by the generation of evacuated chamber. Although this limit is observed to vary between the investigated aerator areas, the trend is not predictable; it is thought that the differences are due to the chaotic mechanisms affecting passive bleeding of the atomizer upon startup and not the effect of aerator area. (c) High liquid flow rates, by the flow limit of the discharge valve. Increasing the ALR acts to further restrict the valve, hence the liquid flow rate continually decreases. The effect of aeration area is not seen to have a significant effect on the discharge limit. Consequently, the operating range corresponding to bubbling is seen to be increased with greater aeration areas [Fig. 8(ii)]. The dependence of bubbling operating range (OR_{bubbling}) in the orifice diameter range considered in the present study is shown as a nonlinear curve plotted in Fig. 8(iii).

4.4 Effect of Mixing Chamber Diameter

The effect of mixing chamber diameter is studied by employing three different diameters of the mixing chamber—14 mm, 20 mm, and 25 mm—for a particular aerator configuration A6A as it is the generic one among the configurations considered in the present study. The effect on other aerator configurations is believed to show the same characteristics as below.

Decreasing the mixing chamber diameter for given input fluid flow rates acts to increase the superficial fluid velocities and Baker parameters throughout the atomizer, including increasing the liquid cross-flow velocity around the aerator periphery. The influence of increasing the liquid cross-flow velocity encourages detachment of the forming bubbles, typically before fully expanded (Balzán et al., 2017).

Figure 9(i) shows the effect of mixing chamber diameter on the internal flow of an effervescent atomizer at a comparable ALR and exit orifice diameter (i.e., discharge nozzle set to fully open). The bubbles produced are visibly seen to decrease in size with reduction in mixing chamber diameter. For the largest mixing chambers (i.e., 20 mm and 25 mm), single bubbling is observed to form a bubbly flow within the mixing chamber. However, at the lowest mixing chamber diameter (i.e., 14 mm), the liquid cross-flow velocity is observed to be sufficient to induce bluff-body recirculation effects, hence bubbles are observed to coalesce in the wake region to form a small void, which sporadically detaches to generate a slug flow. Therefore, despite the reduced bluff-body effect of an ADARPA aerator body design, high superficial Baker parameters are observed to generate unwanted wake effects.

Figure 9(ii) shows the bubbling regions for each case, which were limited at (a) high ALRs, by the transition to jetting regimes. Comparing the investigated extremes (i.e., 14 mm and 25 mm), the mixing chamber diameter is seen to increase the ALR at which transition from bubbling to jetting occurs. This is thought to be due to the increase in liquid cross-flow velocity encouraging detachment of the emerging gas phase. However, the trend is observed to plateau at the smallest mixing chamber diameters (i.e., 14 mm and 20 mm), where transition occurs at comparable ALRs ($\sim 1.0\%$). Despite this, a greater proportion of the bubbling region composed of single bubbling cases with a reduced mixing chamber diameter, with some cases observed at 0.50% ALR for the 14 mm diameter case compared to 0.25% ALR for the 20 mm control configuration for comparable liquid flow rates, is thought to be caused by increased detachment

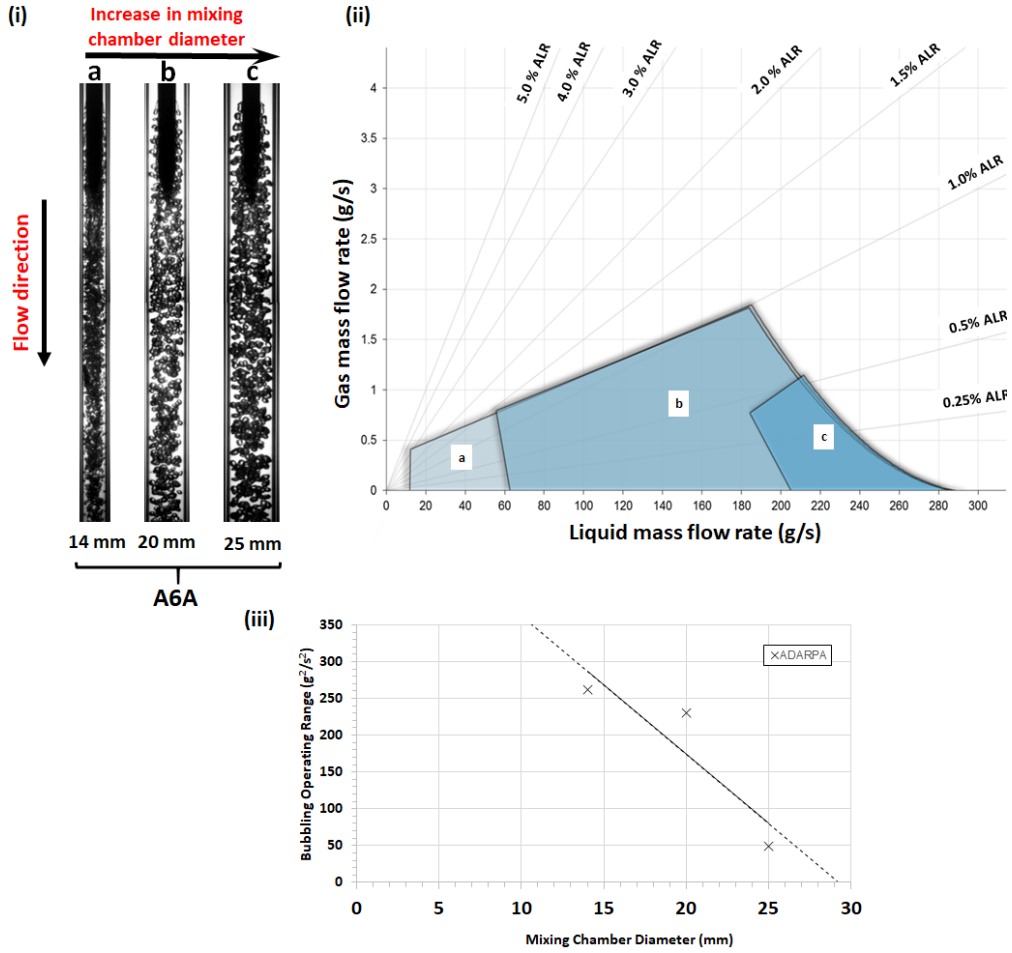

FIG. 9: (i) Comparable observations of varying mixing chamber diameter for A6A: (a) 14 mm diameter, 253 g/s, 0.12% ALR; (b) 20 mm diameter, 251 g/s, 0.12% ALR; (c) 25 mm diameter, 251 g/s, 0.12% ALR. Liquid Baker parameter for all four cases is approximately 802.54 kg/m^{2}s. (ii) Effect of mixing chamber diameter on bubbling operating range, with respect to the fluid mass flow rates: (a) 14 mm diameter; (b) 20 mm diameter; (c) 25 mm diameter. (iii) Dependence of mixing chamber diameter on bubbling operating range.

mechanisms promoting premature bubble detachment. (b) Low liquid flow rates, by the generation of evacuated chamber. The liquid Baker parameter for a given mass flow rate dramatically increases with a reduction in the mixing chamber diameter, the evacuated chamber regime is suppressed, and bubbling is promoted with a reduction in mixing chamber diameter; for example, the liquid Baker parameters at the maximum liquid mass flow rate of 289 g/s are 1890 kg/m^{2}s for the 14 mm diameter and 589 kg/m^{2}s for the 25 mm diameter control configuration. (c) High liquid flow rates, by the flow limit of the discharge valve. Increasing the ALR acts to further restrict the valve, hence the liquid flow rate continually decreases. The dependence of bubbling operating range on mixing chamber diameters (considered in the present study) is shown in Fig. 9(iii).

4.5 Effect of Operating Pressure

The effect of operating pressure on effervescent atomizer internal flow is investigated for 1, 3, and 5 bar with A6A configuration. The characteristics described below are believed to be the same for other configurations as well. A greater operating pressure increases the achievable fluid flow rate through the atomizer; this relates to increased superficial fluid velocities and Baker parameters throughout the atomizer, and therefore is expected to encourage premature detachment of the forming bubbles. In addition, an increased operating pressure acts to compress the gas phase.

Figure 10(i) shows this effect at 0.12% ALR with the discharge nozzle setting fully open (i.e., equivalent exit orifice diameter) in which, as expected, the liquid mass flow rate is observed to increase with greater operating pressures. The bubbles produced from the aerator are visibly seen to decrease in size with increasing operating pressure, which is thought to result from a combination of factors—specifically, increased greater detachment mechanisms (i.e., increased viscous drag and inertia) and increased gas-phase compression. Consequently, in the given cases, the effect of increasing operating pressure is seen to transition the gas injection regimes from p

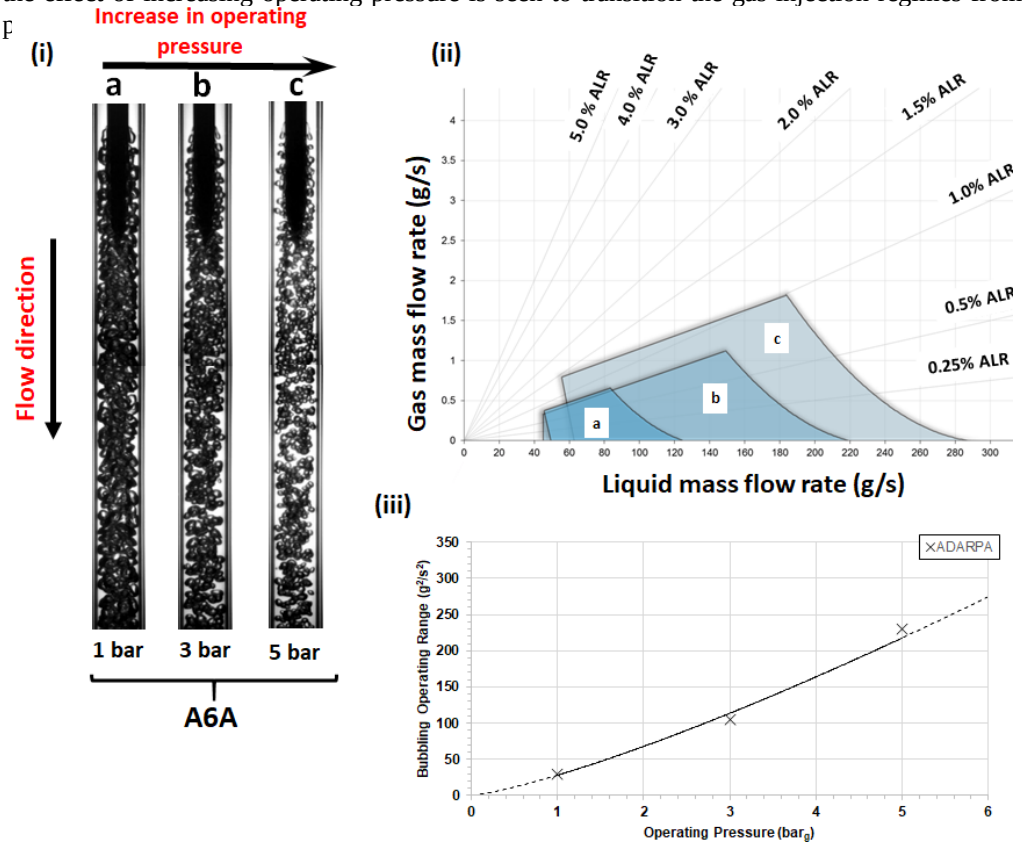

FIG. 10: (i) Comparable observations of varying operating pressure for A6A: (a) 1 bar, 253 g/s, 0.12% ALR; (b) 3 bar, 251 g/s, 0.12% ALR; (c) 5 bar, 251 g/s, 0.12% ALR. Liquid Baker parameter for all four cases is approximately 802.54 kg/m^{2}s. (ii) Effect of operating pressure on bubbling operating range, with respect to the fluid mass flow rates: (a) 1 bar; (b) 3 bar; (c) 5 bar. (iii) Dependence of mixing chamber diameter on bubbling operating range

Figure 10(ii) shows the bubbling regions for both cases, which are limited at (a) high ALRs, by the transition to jetting regimes. Although this limit is observed to occur at an increased ALR for the highest operating pressure, this is not reflected at lower operating pressures, hence a trend cannot be established from the current results. This is similar to the results observed when the flat-end aerator is employed. (b) Low liquid flow rates, by the generation of evacuated chamber. This limit is observed to marginally vary between the investigated operating pressures, which is thought to be caused by the chaotic mechanisms affecting passive bleeding of the atomizer upon startup and not the effect of operating pressure. (c) High liquid flow rates, by the discharge limit of the exit nozzle. Increasing the operating pressure is seen to dramatically increase the discharge limit (i.e., increase the maximum liquid flow rates across all ALRs), where the maximum liquid mass flow rates (and equivalent liquid Baker parameters) for 1 bar_g, 3 bar_g, and 5 bar_g cases at 0% ALR are 130 g/s (413 kg/m^{2}s), 225 g/s (717 kg/m^{2}s), and 289 g/s (923 kg/m^{2}s), respectively. The operating range corresponding to bubbling is seen to increase with operating pressure [considered in the present study; Fig. 10(iii)].

5. CONCLUSION

The present paper is the second of a two-part experimental investigation of effervescent atomizers. The first part dealt with identifying the advantages of employing streamlined aerator design over the conventional flat-end type of aerator. In addition, it was shown that DARPA SUBOFF afterbody design for streamlining the aerator was the best among the four different types of streamline designs investigated. This paper is the continuation of the previous part. Here, detailed characterization of the internal flow and resulting spray characteristics at the nozzle exit of the novel DARPA SUBOFF afterbody design aerator was carried out and reported for the first time.

The internal flow was imaged by employing high-speed shadowgraphy to study the effect of ALR on it. The resulting droplet size and velocity were determined using PDA. As evidenced by the past studies, the study of internal flow of atomizers form an essential part of studying their performance.

The ALR was systematically increased in the range of 0–5% to study its effect on internal flow. It was observed that the gas injection regime (at the aerator orifice) transited in mechanisms to produce bubbles and jets, and finally led to an evacuated chamber. The corresponding effect on the two-phase flow in the mixing chamber was observed to produce a transition from bubbly flow to slug flow to churn flow and finally to annular flow. The droplet size (AMD: D10) at the center decreased from $\sim$ 150 μm to 50–80 μm when ALR was increased from 0.12% to 1.5%. The corresponding droplet velocities increased from $\sim$ 35 m/s to 50 m/s within the same ALR range.

Other operating parameters investigated were operating pressure (1–5 bar), aerator orifice diameter (0.75 mm–3 mm), aeration area (1.77 mm^2–14.4 mm^2), and mixing chamber diameter (14 mm, 20 mm, and 25 mm). Within these conditions a parameter called bubbling operating range (OR_{bubbling}) was determined, which quantified the range of corresponding operating conditions in which the much desired bubbly flow in the effervescent atomizers is observed. Within the abovementioned range of different operating parameters the dependence of OR_{bubbling} was as follows:

- OR_{bubbling} increased with a decrease in aerator orifice diameter.
- OR_{bubbling} increased nonlinearly with an increase in aeration areas.

- OR_{bubbling} decreased with an increase in mixing chamber diameter.
- OR_{bubbling} increased with an increase in operating pressure.

These relations are believed to be very useful for modelers trying to simulate the internal flow of effervescent atomizers using DARPA SUBOFF afterbody design.

REFERENCES

Balzán, M.A., Sanders, R.S., and Fleck, B.A., Bubble Formation Regimes during Gas Injection into a Liquid Cross Flow in a Conduit, *Can. J. Chem. Eng.*, vol. **95**, no. 2, pp. 372–385, 2017.

Bhagwat, S.M., Study of Flow Patterns and Void Fractions in Vertical Downward Two Phase Flow, PhD, Oklahoma State University, 2011.

Broniarz-Press, L., Ochowiak, L.M., and Woziwodzki, S., Atomization of PEO Aqueous Solutions in Effervescent Atomizers, *Int. J. Heat Fluid Flow*, vol. **31**, no. 4, pp. 651–658, 2010.

Buckner, H.N. and Sojka, P.E., Effervescent Atomization of High-Viscosity Fluids. Part I: Newtonian Liquids, *Atomization Sprays*, vol. **1**, no. 3, pp. 239–252, 1991.

Buckner, H.E. and Sojka, P.E., Effervescent Atomization of High Viscosity Fluids. Part II: Non-Newtonian Liquids, *Atomization Sprays*, vol. **3**, pp. 157–170, 1993.

Catlin, C.A. and Swithenbank, J., Physical Processes Influencing Effervescent Atomizer Performance in the Slug and Annular Flow Regimes, *Atomization Sprays*, vol. **11**, no. 5, pp. 575–595, 2001.

Chen, S.K. and Lefebvre, A.H., Spray Cone Angles of Effervescent Atomizers, *Atomization Sprays*, vol. **4**, no. 3, pp. 275–290, 1994.

Chen, S.K., Lefebvre, A.H., and Rollbuhler, J., Influence of Ambient Air Pressure on Effervescent Atomization, *J. Propuls. Power*, vol. **9**, no. 1, pp. 10–15, 1993.

Cheung, S.C.P., Yeoh, G.H., Qi, F.S., and Tu, J.Y., Classification of Bubbles in Vertical Gas-Liquid Flow: Part 2—A Model Evaluation, *Int. J. Multiphase Flow*, vol. **39**, pp. 135–147, 2012.

Chin, J.S. and Lefebvre, A.H., A Design Procedure for Effervescent Atomizers, *J. Eng. Gas Turbines Power*, vol. **117**, no. 2, pp. 266–271, 1995.

Chin, J.S. and Lefebvre, A.H., Flow Regimes in Effervescent Atomization, *Atomization Sprays*, vol. **3**, no. 4, pp. 463–475, 1993.

BSA Flow Software, Installation and User's Guide, Dantec Dynamics, 4.10 ed., 2006.

Forrester, S.E. and Rielly, C.D., Bubble Formation from Cylindrical, Flat and Concave Sections Exposed to a Strong Liquid Cross-Flow, *Chem. Eng. Sci.*, vol. **53**, no. 8, pp. 1517–1527, 1998.

Furukawa, T. and Fukano, T., Effects of Liquid Viscosity on Flow Patterns in Vertical upward Gas-Liquid Two-Phase Flow, *Int. J.Multiphase Flow*, vol. **27**, no. 6, pp. 1109–1126, 2001.

Geckler, S.C. and Sojka, P.E., Effervescent Atomization of Viscoelastic Liquids: Experiment and Modeling, *J. Fluids Eng., Transact. ASME*, vol. **130**, no. 6, p. 061303, 2008.

Gomez, J., Influence of Bubble Size on an Effervescent Atomization, PhD, University of Alberta, 2010.

Hampel, U., Othal, J., Boden, S., Beyer, M., Schleicher, E., Zimmermann, W., and Jicha, M., Miniature Conductivity Wire-Mesh Sensor for Gas-Liquid Two-Phase Flow Measurement, *Flow Measure. Instrument.*, vol. **20**, no. 1, pp. 15–21, 2009.

Hong, M., Fleck, B.A., and Nobes, D.S., Unsteadiness of the Internal Flow in an Effervescent Atomizer Nozzle, *Exp. Fluids*, vol. **55**, no. 12, pp. 1–15, 2014.

Huang, X., Wang, X.S., and Liao, G.X., Visualization of Two Phase Flow inside an Effervescent Atomizer, *J. Visualization*, vol. **11**, no. 4, pp. 299–308, 2008.

Huang, X., Wang, X.S., and Liao, G.X., Characterization of an Effervescent Atomization Water Mist Nozzle and Its Fire Suppression Tests, *Proc. Combust. Inst.*, vol. **33**, no. 2, pp. 2573–2579, 2011.

Jagannathan, T.K., Nagarajan, R., and Ramamurthi, K., Effect of Ultrasound on Bubble Breakup within the Mixing Chamber of an Effervescent Atomizer, *Chem. Eng. Process. Process Intens.*, vol. **50**, no. 3, pp. 305–315, 2011.

Jedelsky, J., Jicha, M., and Slama, J., Characterization of Spray Generated by Multihole Effervescent Atomizer and Comparison with Standard Y-Jet Atomizer, *Proc. of the Ninth Int. Conf. on Liquid Atomization and Spray Systems (ICLASS-2003)*, Sorrento, Italy, 2003.

Jedelsky, J., Landsmann, M., Jicha, M., and Kuritka, I., Effervescent Atomizer: Influence of the Operation Conditions and Internal Geometry on Spray Structure: Study Using PIV-PLIF, *Proc. of ILASS*, Como Lake, Italy, 2008.

Jedelsky, J., Miroslav, J., Slama, J., and Otahal, J., Development of an Effervescent Atomizer for Industrial Burners, *Energy Fuels*, vol. **23**, no. 12, pp. 6121–6130, 2009.

Jedelsky, J. and Jicha, M., Energy Conversion during Effervescent Atomization, *Fuel*, vol. **111**, pp. 836–844, 2013.

Jedelsky, J. and Jícha, M., Spray Characteristics and Liquid Distribution of Multi-Hole Effervescent Atomizers for Industrial Burners, *Appl. Therm. Eng.*, vol. **96**, pp. 286–296, 2016.

Jobehdar, M.H., Experimental Study of Two-Phase Flow in a Liquid Cross-Flow and an Effervescent Atomizer, PhD, University of Western Ontario, 2014.

Kim, J.Y. and Lee, S.Y., Dependence of Spraying Performance on the Internal Flow Pattern in Effervescent Atomizers, *Atomization Sprays*, vol. **11**, no. 6, pp. 735–756, 2001.

Konstantinov, D.D., Effervescent Atomization for Complex Fuels Including Bio-Fuels, PhD, University of Wales, 2012.

Laakkonen, M., Alopaeus, V., and Aittamaa, J., Validation of Bubble Breakage, Coalescence and Mass Transfer Models for Gas-Liquid Dispersion in Agitated Vessel, *Chem. Eng. Sci.*, vol. **61**, no. 1, pp. 218–228, 2006.

Lörcher, M., Schmidt, F., and Mewes, D., Effervescent Atomization of Liquids, *Atomization Sprays*, vol. **15**, no. 2, pp. 145–168, 2005.

Lefebvre, A.H., A Novel Method of Atomization with Potential Gas Turbine Application, *Def. Sci. J.*, vol. **38**, pp. 353–361, 1988.

Lefebvre, A.H., Wang, X.F., and Martin, C.A., Spray Characteristics of Aerated-Liquid Pressure Atomizers, *J. Propuls. Power*, vol. **4**, no. 4, pp. 293–298, 1988.

Lefebvre, A.H. and Chen, S.K., Discharge Coefficients for Plain-Orifice Effervescent Atomizers, *Atomization Sprays*, vol. **4**, no. 3, pp. 275–290, 1994.

Lefebvre, A.H., Some Recent Developments in Twin-Fluid Atomization, *Part. Part. Syst. Char.*, vol. **13**, no. 3, pp. 205–216, 1996.

Liao, Y. and Lucas, D., A Literature Review on Mechanisms and Models for the Coalescence Process of Fluid Particles, *Chem. Eng. Sci.*, vol. **65**, no. 10, pp. 2851–2864, 2010.

Liu, M., Duan, Y., and Zhang, T., Evaluation of Effervescent Atomizer Internal Design on the Spray Unsteadiness Using a Phase/Doppler Particle Analyzer, *Exp. Therm. Fluid Sci.*, vol. **34**, no. 6, pp. 657–665, 2010.

Liu, M., Duan, Y., Zhang, T., and Xu, Y., Evaluation of Unsteadiness in Effervescent Sprays by Analysis of Droplet Arrival Statistics—The Influence of Fluids Properties and Atomizer Internal Design, *Exp. Therm. Fluid Sci.*, vol. **35**, no. 1, pp. 190–198, 2011.

Loebker, D. and Empie, H.J., High Mass Flow-Rate Effervescent Spraying of High Viscosity Newtonian

Liquid, *Proceedings of the 10th Annual Conf. on Liquid Atomization and Spray Systems*, Ottawa, ON, pp. 253–257, 1997.

Lörcher, M. and Mewes, D., Atomization of Liquids by Two-Phase Gas-Liquid Flow through a Plain-Orifice Nozzle: Flow Regimes inside the Nozzle, *Chem. Eng. Technol.*, vol. **24**, no. 2, pp. 167–172, 2001.

Loubière, K., Castaignede, V., Hebrard, G., and Roustan, M., Bubble Formation at a Flexible Orifice with Liquid Cross-Flow, *Chem. Eng. Process. Process Intens.*, vol. **43**, no. 6, pp. 717–725, 2004.

Ma, X., Duan, Y., and Liu, M., Atomization of Petroleum-Coke Sludge Slurry Using Effervescent Atomizer, *Exp. Therm. Fluid Sci.*, vol. **46**, pp. 131–138, 2013.

Mlkvik, M., Stahle, P., Schuchmann, H.P., Gaukel, V., Jedelsky, J., and Jicha, M., Twin-Fluid Atomization of Viscous Liquids: The Effect of Atomizer Construction on Breakup Process, Spray Stability and Droplet Size, *Int. J. Multiphase Flow*, vol. **77**, pp. 19–31, 2015.

Mostafa, A., Fouad, M., Enayet, M., and Osman, S., Measurements of Spray Characteristics Produced by Effervescent Atomizers, *40th AIAA/ASME/SAE/ASEE Joint Propulsion Conf. and Exhibit*, Fort Lauderdale, FL, 2004.

Nielsen, A.F., Poul, B., Kristensen, H.G., Kristensen, J., and Hovgaard, L., Investigation and Comparison of Performance of Effervescent and Standard Pneumatic Atomizer Intended for Soluble Aqueous Coating, *Pharmaceut. Dev. Technol.*, vol. **11**, no. 2, pp. 243–253, 2006.

Niland, A., Internal Flow Studies for the Characterisation and Optimisation of an Effervescent Atomizer, PhD, Cardiff University, 2017.

Ochowiak, M., Broniarz-Press, L., and Rozanski, J., The Discharge Coefficient of Effervescent Atomizers, *Exp. Therm. Fluid Sci.*, vol. **34**, no. 8, pp. 1316–1323, 2010.

Ochowiak, M., The Effervescent Atomization of Oil-in-Water Emulsions, *Chem. Eng. Proces.: Process Intens.*, vol. **52**, pp. 92–101, 2012.

Ochowiak, M., Broniarz-Press, L., Rozanska, S., and Rozanski, J., The Effect of Extensional Viscosity on the Effervescent Atomization of Polyacrylamide Solutions, *J. Indust. Eng. Chem.*, vol. **18**, no. 6, pp. 2028–2035, 2012.

Panchagnula, M.V. and Sojka, P.E., Spatial Droplet Velocity and Size Profiles in Effervescent Atomizer-Produced Sprays, *Fuel*, vol. **78**, no. 6, pp. 729–741, 1999.

Petersen, F.J., Worts, O., Schaefer, T., and Sojka, P.E., Design and Atomization Properties for an Inside-Out Type Effervescent Atomizer, *Drug Dev. Indust. Pharm.*, vol. **30**, no. 3, pp. 319–326, 2004.

Petersen, F.J., Worts, O., and Sojka, P.E., Effervescent Atomization of Aqueous Polymer Solutions and Dispersions, *Pharm. Dev. Technol.*, vol. **6**, no. 2, pp. 201–210, 2001.

Rahman, M.A., Balzan, M., Heidrick, T., and Fleck, B.A., Effects of the Gas Phase Molecular Weight and Bubble Size on Effervescent Atomization, *Int. J. Multiphase Flow*, vol. **38**, no. 1, pp. 35–52, 2012.

Ramamurthi, K., Sarkar, U.K., and Raghunandan, B.N., Performance Characteristics of Effervescent Atomizer in Different Flow Regimes, *Atomization Sprays*, vol. **19**, no. 1, pp. 41–56, 2009.

Rigby, G.D., Evans, G.M., and Jameson, G.J., Modelling of Gas Flow from a Submerged Orifice in Liquid Cross-Flow, *Chem. Eng. Res. Design*, vol. **73**, no. A3, pp. 234–240, 1995.

Roesler, T.C. and Lefebvre, A.H., Studies on Aerated-Liquid Atomization, *Int. J. Turbo Jet Eng.*, vol. **6**, nos. 3-4, pp. 221–229, 1989.

Roesler, T.C. and Lefebvre, A.H., Photographic Studies on Aerated Liquid Atomization, Combustion Fundamentals and Applications, *Proc. of the Meeting of the Central States Section of the Combustion Institute*, Indianapolis, Indiana, 1988.

Santangelo, P.J. and Sojka, P.E., A Holographic Investigation of the Near-Nozzle Structure of an Effervescent Atomizer-Produced Spray, *Atomization Sprays*, vol. **5**, no. 2, pp. 137–155, 1995.

Schröder, J., Kraus, S., Rocha, B.B., Gaukal, V., and Schuchmann, H.P., Characterization of Gelatinized Corn Starch Suspensions and Resulting Drop Size Distributions after Effervescent Atomization, *J. Food Eng.*, vol. **105**, no. 4, pp. 656–662, 2011.

Schröder, J., Kleinhans, A., Serfert, Y., Drusch, S., Karbstein, H.P., and Gaukel, V., Viscosity Ratio: A Key Factor for Control of Oil Drop Size Distribution in Effervescent Atomization of Oil-in-Water Emulsions, *J. Food Eng.*, vol. **111**, no. 2, pp. 265–271, 2012.

Sen, D., Balzan, M.A., Nobes, D.S., and Fleck, B.A., Bubble Formation and Flow Instability in an Effervescent Atomizer, *J. Visualization*, vol. **17**, no. 2, pp. 113–122, 2014.

Shinnar, R. and Church, J.M., Statistical Theories of Turbulence in Predicting Particle Size in Agitated Dispersions, *Indust. Eng. Chem.*, vol. **52**, no. 3, pp. 253–256, 1960.

Sojka, P.E. and Lefebvre, A.H., A Novel Method of Atomizing Coal-Water Slurry Fuels, US DOE, Pittsburgh, Tech. Rep. DOE/PC/79913-T4, May 1990.

Sojka, P.E. and Buckner, H.N., Effervescent Atomization of High-Viscosity Fluids. Part II: Non-Newtonian Liquids, *Atomization Sprays*, vol. **3**, no. 2, pp. 157–170, 1993.

Sovani, S.D., Sojka, P.E., and Lefebvre, A.H., Effervescent Atomization, *Prog. Energy Combust. Sci.*, vol. **27**, no. 4, pp. 483–521, 2001.

Sovani, S.D., Chou, E., Sojka, P.E., Gore, J.P., Eckerle, W.A., and Crofts, J.D., High Pressure Effervescent Atomization: Effect of Ambient Pressure on Spray Cone Angle, *Fuel*, vol. **80**, no. 3, pp. 427–435, 2001.

Sovani, S.D., Crofts, J.D., Sojka, P.E., Gore, J.P., and Eckerle, W.A., Structure and Steady-State Spray Performance of an Effervescent Diesel Injector, *Fuel*, vol. **84**, nos. 12-13, pp. 1503–1514, 2005.

Stähle, P., Gaukel, V., and Schuchmann, H.P., Investigation on the Applicability of the Effervescent Atomizer in Spray Drying of Foods: Influence of Liquid Viscosity on Nozzle Internal Two-Phase Flow and Spray Characteristics, *J. Food Process Eng.*, vol. **38**, no. 5, pp. 474–487, 2015a.

Stähle, P., Gaukel, V., and Schuchmann, H.P., Comparison of an Effervescent Nozzle and a Proposed Air-Core-Liquid-Ring (ACLR) Nozzle for Atomization of Viscous Food Liquids at Low Air Consumption, *J. Food Process Eng.*, vol. **40**, no. 1, p. E12268, 2015b.

Sun, C., Ning, Z., Lv, M., Yan, K., and Fu, J., Time-Frequency Analysis of Acoustic and Unsteadiness Evaluation in Effervescent Sprays, *Chem. Eng. Sci.*, vol. **127**, pp. 115–125, 2015.

Sutherland, J.J., Sojka, P.E., and Plesniak, M.W., Ligament-Controlled Effervescent Atomization, *Atomization Sprays*, vol. **7**, no. 4, pp. 383–406, 1997.

Tse, K., Martin, T., Mcfarlane, C.M., and Nienow, A.W., Visualisation of Bubble Coalescence in a Coalescence Cell, a Stirred Tank and a Bubble Column, *Chem. Eng. Sci.*, vol. **53**, no. 23, pp. 4031–4036, 1998.

Usui, K. and Sato, K., Vertically Downward Two-Phase Flow, (I) Void Distribution and Average Void Fraction, *J. Nucl. Sci. Technol.*, vol. **26**, no. 7, pp. 670–680, 1989.

Vanderwege, B.A. and Hochgreb, S., The Effect of Fuel Volatility on Sprays from High-Pressure Swirl Injectors, *Symp. (Int.) Combust.*, vol. **27**, no. 2, pp. 1865–1871, 1998.

Wade, R.A., Weerts, J.M., Gore, J.P., and Eckerle, W.A., Effervescent Atomization at Injection Pressures in the MPa Range, *Atomization Sprays*, vol. **9**, no. 6, pp. 651–667, 1999.

Whitlow, J.D. and Lefebvre, A.H., Effervescent Atomizer Operation and Spray Characteristics, *Atomization Sprays*, vol. **3**, no. 6, pp. 137–155, 1993.

Yang, G.Q., Du, B., and Fan, L.S., Bubble Formation and Dynamics in Gas-Liquid-Solid Fluidization—A Review, *Chem. Eng. Sci.*, vol. **62**, nos. 1-2, pp. 2–27, 2007.

Zhou, J., Flow Patterns in Vertical Air/Water Flow with and without Surfactant, PhD, University of Dayton, 2013.